

## Control structure selection for four-product Petlyuk column

Deeptanshu Dwivedi<sup>a</sup>, Ivar J. Halvorsen<sup>b</sup>, Sigurd Skogestad<sup>a,\*</sup>

<sup>a</sup> Department of Chemical Engineering, Norwegian University of Science and Technology, N-7491 Trondheim, Norway

<sup>b</sup> SINTEF ICT, Applied Cybernetics, N-7465 Trondheim, Norway

### ARTICLE INFO

#### Article history:

Received 13 March 2012  
Received in revised form 30 June 2012  
Accepted 23 July 2012  
Available online 31 July 2012

#### Keywords:

Energy efficient distillation  
Thermally coupled distillation  
Control structure design  
Divided wall columns  
Petlyuk column

### ABSTRACT

Direct material coupling between column sections in distillation leads to energy efficient systems like the Petlyuk column but with more difficult control problems compared to conventional multicomponent distillation sequences. A control study of a four-product extended Petlyuk column operating close to minimum energy is reported here. We study the “ideal” case with all steady state degrees of freedom available for control, including the vapor split valves, which is required to achieve minimum energy under all conditions. Four decentralized control structures are proposed and tested against a wide range of disturbances. This work demonstrates also the use of the graphical  $V_{min}$  tool which can be used to visualize the minimum boilup requirement for Petlyuk arrangements.

© 2012 Elsevier B.V. All rights reserved.

### 1. Introduction

Significant energy losses in conventional distillation sequences result from internal remixing. This can be reduced greatly by direct material coupling and by doing easiest split first. Petlyuk et al. [1] proposed such a scheme to separate feed into three products, using a prefractionator. The prefractionator is designed and operated to do the easiest split first. A similar scheme was shown in a patent by Cahn and DiMiceli [2]. Stupin [3] claimed significant energy and capital saving using thermally coupled arrangement with a prefractionator. Such prefractionator arrangements can also be implemented in a single column shell using a dividing wall [4]. The German company BASF reports more than 100 industrial installations [5] of divided wall columns for separation of a feed into three products.

The idea of Petlyuk to separate a mixture to three products can be extended to separate a feed mixture into four products in a “four-product extended Petlyuk column”. Such systems may offer further energy savings [6]. While several control studies have been reported on three-product divided wall columns and four-product Kaibel columns, there are no control studies reported on four-product extended Petlyuk columns.

Wolff and Skogestad [7] did a steady state study and operability analysis on a three-product Petlyuk column and conclude that the simultaneous specification of both impurities in the side product may be infeasible. Further, the liquid and vapor split ratios between

prefractionator and the main column should be manipulated to get the optimal energy benefits. Niggemann et al. [8] conducted simulation and experimental studies for separation of a mixture of fatty alcohols into three high-purity products. They reported that the heat transfer across the dividing wall can be a factor in design and operation. Lestak et al. [9] argued that there may be some beneficial regions and the heat transfer across the dividing wall, should help decrease the overall energy consumptions. In non-beneficial regions however, the wall should be insulated. Mutalib et al. [10] reported experimental studies conducted on pilot plant and showed a two point control of the system. Ling and Luyben [11] explained that the liquid split valve must be manipulated and proposed a control structure with the use of four composition loops with the liquid split controlling the heavy key at the top stage of the prefractionator. Kiss and Bildea [12] gave some general control perspectives on dividing-wall columns. Ling et al. [13] suggested a control structure that can avoid remixing of intermediates leading to energy optimal operation. van Diggelen et al. [14] reported a study on dividing-wall columns giving emphasis on the controllability properties and dynamic responses. Some more works on the use of Model Predictive Control have been reported for divided wall columns [15–17].

Olujić et al. [18] reported recent advances on column internals for divided wall columns. Dejanović et al. [5] reported simple design procedures for separating multicomponent aromatic mixtures into four products using energy efficient multiple partitioned dividing wall arrangements.

In this paper we report the very first work on control of a four-product extended Petlyuk column. We study, here the separation of A (methanol), B (ethanol), C (propanol) and D (*n*-butanol) using the

\* Corresponding author. Tel.: +47 735 94154; fax: +47 735 94080.  
E-mail address: [skoge@ntnu.no](mailto:skoge@ntnu.no) (S. Skogestad).

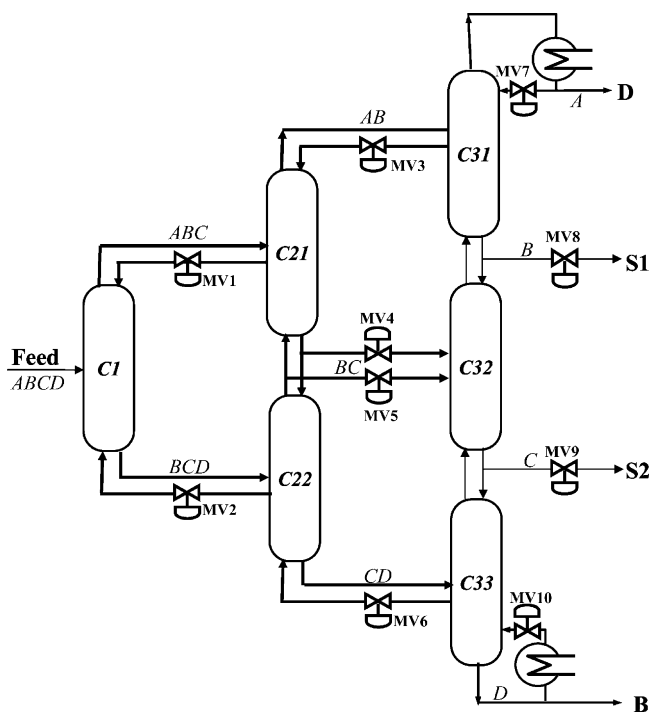


Fig. 1. Four-product extended Petlyuk arrangement.

four-product extended Petlyuk arrangement. For this case study, the energy saving is about 50% compared to the conventional direct and indirect sequences [19].

Fig. 1 shows the schematic of a four-product extended Petlyuk column. There are a total of six sub-columns making the Petlyuk arrangement and are numbered as C1, C21, C22, C31, C32 and C33 for convenience. This arrangement can also be fabricated in a single column shell using a double wall partition [19], as shown in Fig. 2. Thermodynamically, the arrangements shown in Figs. 1 and 2 are equivalent. We shall refer to the arrangement shown in Fig. 1 for the rest of the discussion.

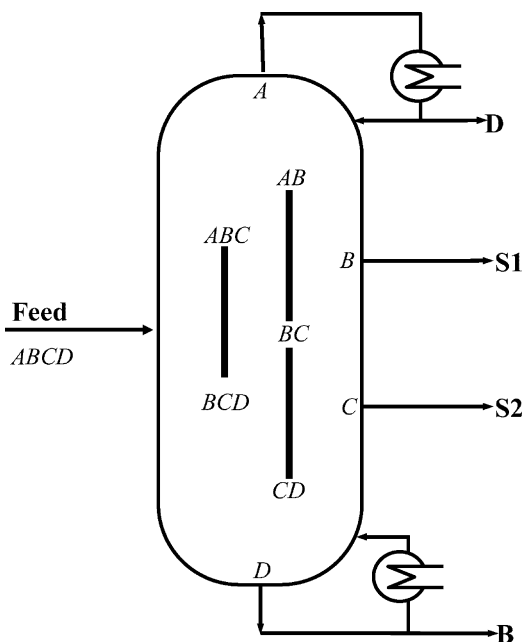


Fig. 2. Dividing-wall implementation: four-product extended Petlyuk arrangement in single column shell using double wall partition.

Table 1  
Model details: four-product Petlyuk column.

Relative volatilities [ABCD]	[7.1 4.43 2.15 1]
Number of stages in C1	30 + 30
Number of stages in C21	30 + 30
Number of stages in C22	30 + 30
Number of stages in C31	30 + 30
Number of stages in C32	30 + 30
Number of stages in C33	30 + 30
Feed flow rate (mol/min)	1
Feed composition	Equimolar
Nominal purity of distillate ( $x_D^D$ )	99.55 (mol%)
Nominal purity of upper side product ( $x_{S1}^B$ )	99.33 (mol%)
Nominal purity of lower side product ( $x_{S2}^C$ )	99.56 (mol%)
Nominal purity of bottom product ( $x_B^D$ )	99.62 (mol%)

In this study, we assume *ten* degrees of freedom (valves) available for composition control. The feed rate and feed conditions are assumed given. The distillate and the bottoms flow are used for level control of condenser and reboiler, respectively, while the condenser duty is used for the pressure control. We assume adiabatic column sections, i.e., no heat transfer across the walls.

Note that we have included three vapor distribution valves (MV2, MV4 and MV6) as manipulated valves. This is unconventional [20] but can be implemented in real systems and development of vapor split valves for dividing-wall columns can be an area for future research as this can help to attain minimum energy usage when there are feed composition disturbances or changes in product specifications. A prototype of vapor split valves was demonstrated experimentally on a pilot plant recently [21]. Note that the valves, MV1, MV2, MV3, MV4, MV5, MV6, MV8 and MV9 (see Fig. 1) do not specify direct molar flow rates, but are modeled as split ratios in the dynamic model. For example MV1 in Fig. 1 manipulates ratio of liquid drawn out from sub-column C21 to the total molar liquid flow in sub-column C21.

We consider the separation of components A (lightest), B, C and D (heaviest). However, note that the letters B and D are also used to denote the bottom and distillate (top) products, respectively. To reduce the confusion, we will use subscripts for components and superscripts for products. For example,  $x_B^D$  denotes the mole fraction of component B in product D.

## 2. Case study

The data is given in Table 1. The process is modeled in Matlab using the simplifying assumptions of constant relative volatility and constant molar flows in each column section. The four components A, B, C and D have relative volatilities similar to the mixture of methanol, ethanol, propanol and *n*-butanol. We assume constant pressure, negligible vapor holdup, a total condenser and equilibrium on all stages. We assume linearized liquid flow dynamics. Compared to the specified purities given in Table 1, a large number of stages is assumed in each sub-column. This implies that the used energy for a near-sharp separation is close to the minimum energy using an infinite number of stages.

### 2.1. Steady state composition profiles

Fig. 3 shows composition profiles at nominal steady state conditions of components A (methanol), B (ethanol), C (propanol) and D (*n*-butanol) in different sub-columns of the Petlyuk arrangement.

In a Petlyuk arrangement, the easiest separation is carried out first. The more difficult splits, i.e., the splits between the immediate boiling components are carried out last. In the first sub-column C1, the easy split is between A and D, whereas the intermediate components, B and C, distribute in both products. The key impurity in the top stage of sub-column C1 is D and the key impurity in C1

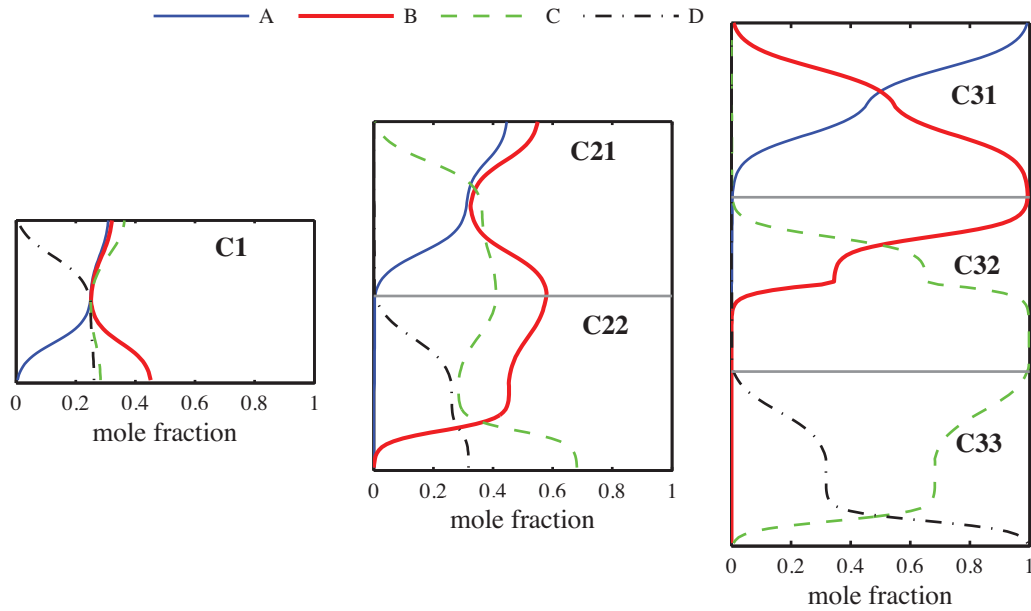


Fig. 3. Steady state composition profiles in sub-columns C1, C21, C22, C31, C32 and C33.

bottoms is A. The feed to sub-column C21 is A, B and C. The easy split is between A and C, where B is allowed to distribute to both ends of sub-column C21. The key impurity at C21 top stage is C and the key impurity at C21 bottom stage is A.

The more difficult binary splits are done in sub-columns C31, C32 and C33. Sub-column C31 does the split between the two light components, A and B, sub-column C32 does the B/C split and sub-column C33 does the C/D split.

### 3. $V_{min}$ diagrams

Halvorsen and Skogestad [22] have developed a graphical tool, the “ $V_{min}$ ” diagrams, to visualize the minimum energy requirement for sharp and non-sharp separations. For separation of ideal multicomponent mixtures the Underwood equations [23] are effective for generating the  $V_{min}$  diagrams, but the  $V_{min}$  diagram may also be generated for non-ideal mixtures using simulations with rigorous thermodynamic models [24].

Fig. 4 shows the  $V_{min}$  diagram for an equimolar A–B–C–D mixture with a liquid feed. The y-axis shows the normalized minimum boilup ( $V/F$ ) and the x-axis shows the net product withdrawal ( $D/F$ ) in a conventional two-product column. Since, we are studying near-sharp separations, the peak points denoted by  $P_{AB}$ ,  $P_{AC}$ ,  $P_{AD}$ ,  $P_{BC}$ ,  $P_{BD}$  and  $P_{CD}$  are of interest. The peak  $P_{AB}$  gives the minimum vapor flow ( $V/F$ ), required for separating A and B. Note that the corresponding product split ( $x$ -coordinate)  $D/F=0.25$ , since the feed is equimolar. Similarly point  $P_{AD}$  denotes the minimum vapor required to separate A and D.

Minimum energy is achieved when the prefractionator sub-columns C1, C21 and C22 are operated at their “preferred splits”, denoted by points  $P_{AD}$ ,  $P_{AC}$  and  $P_{BD}$ , respectively. Thus, the internal flows in the sub-columns can directly be obtained from the  $V_{min}$  diagram. This can be used for the short cut design and preliminary sizing of column sections [19,25]. In addition, with the minimum flows required for separation known, flows in a more detailed dynamic model for the process can be initialized.

Halvorsen and Skogestad [26] and Fidkowski and Królikowski [27] showed that in a Petlyuk arrangement, the minimum energy

requirement to separate a multi-component feed is equal to the “most difficult binary separation”.

$$V_{min, Petlyuk} = \max(V_{AB}, V_{BC}, V_{CD}) \quad (1)$$

Here,  $V_{AB}$ ,  $V_{BC}$  and  $V_{CD}$  are the minimum boilup required for sharp separation of A/BCD, AB/CD and ABC/D in a conventional two-product distillation column with A–B–C–D feed. Note that,  $V_{AB}$ ,  $V_{BC}$  and  $V_{CD}$  depend on the feed conditions.

In Fig. 4, the  $P_{CD}$  peak is the highest. This implies that the separation of C and D is the most difficult binary split in terms of energy usage. Thus, the minimum boilup required for sharp separation of the multicomponent feed using a Petlyuk arrangement is equal to the boilup required for this binary split ( $=V_{CD} = V_B^{33}$  in Fig. 4).

In a generalized Petlyuk arrangement, the minimum vapor flow in sub-columns above and below a side product may be different. This is equal to the difference in the heights of the peaks in the  $V_{min}$  diagram. A different vapor distribution in sub-columns can be realized by drawing side products as both liquid and vapor or,

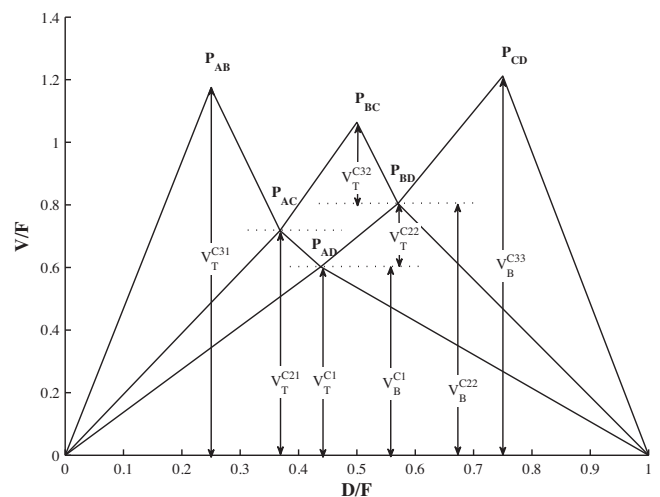
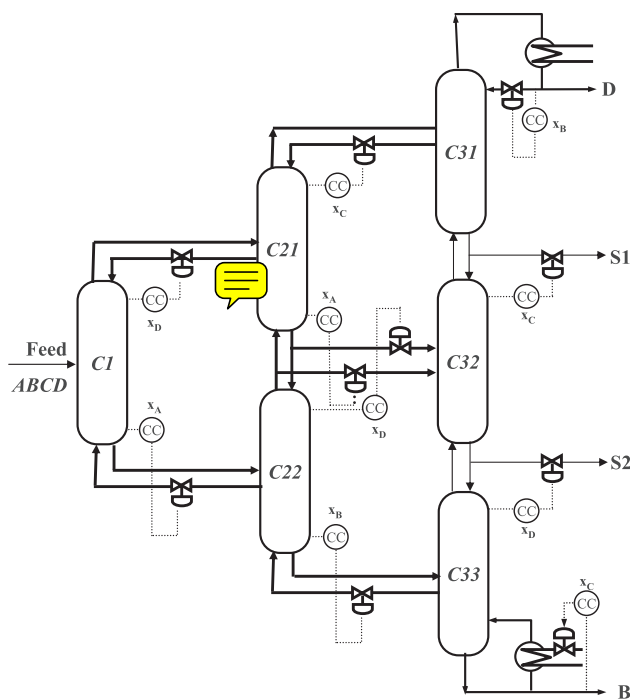


Fig. 4.  $V_{min}$  diagram showing minimum vapor flows in various sections required for sharp separation of equimolar A–B–C–D feed.



**Fig. 5.** Proposed control structures for three-product Petlyuk columns. In pre-fractionator controller, XC can be a temperature controller [28] or a composition controller for the key impurity in the least pure end [29,30], i.e., heavy key  $x_C$  at  $C1^{TOP}$  [11,31] or, light key  $x_A$  at  $C1^{BOT}$ .

alternatively, by using an intermediate heater or cooler between sub-columns. In this study, only liquid products are drawn and internal flows in sections C31 and C32 are recalculated for this more practical design. This modification does not lead to any additional energy requirements for a given separation, but it may allow for “over-purification” in some sections.

#### 4. Control structures for three-product Petlyuk columns

Before we discuss the control structures for the four-product Petlyuk column, we present a short note based on the works published by previous workers [11,28–31] on the control structure design of three-product Petlyuk column. Fig. 5 shows a general control structure for the three-product Petlyuk column with a ternary feed of A, B and C for the conventional case when the vapor split is not used for control.

To achieve the desired purity of the side stream (S) in the main column, the A/C split in the pre-fractionator (C1) must be controlled to avoid that too much C goes in the top or too much A goes in the bottom. The specifications for the split in the pre-fractionator (maximum values for  $x_C$  at  $C1^{TOP}$  and  $x_A$  at  $C1^{BOT}$ ) are indirectly determined by the purity specifications for the side stream (S). With a fixed vapor split ( $R_V$ ) one cannot control both at the same time, which is why Christiansen [29] and Halvorsen and Skogestad [30] propose to control the key impurity in the least pure end. Ling and Luyben [11], Kiss and Rewagad [31] propose to control  $x_C$  in the top of the pre-fractionator, which will be the best policy provided the top is the least pure end (i.e., when breakthrough of component A in the bottom of the pre-fractionator (C1) is not a problem).

We can now discuss the control of the final products (D, S, B) in the main column. For the distillate (D) and bottoms (B) product it is usually simple. These products have only one impurity each (the amount of B component), so for these we simply control the impurity ( $x_B$  in distillate (D) and  $x_B$  in bottoms (B)). However, for

the side stream S, there are two impurities (components A and C), and we do not have enough degrees of freedom to control both.

One solution is to control the more “difficult” of the two and let the other be over-purified. For example, if the B/C split is more difficult than the A/B split, then one should control the amount of C in the side stream ( $x_C^S$ ). This is proposed by Ling and Luyben [11] and if we look at the vapor–liquid equilibria data of the components they studied, then we indeed find that toluene (B)/*o*-xylene (C) is the more difficult separation. However, what would happen if the feed conditions change so that the benzene (A)/toluene (B) split becomes the difficult one and we get too much A in the side product? To avoid this, we would need to increase the vapor flow in the top section C21, and since the vapor flow is the same in sections C21 and C22 we would get excess vapor in the bottom section C22. We resolve a similar issue in the four-product Petlyuk column by our proposed decentralized control structures described below.

#### 5. Proposed control structures for the four-product extended Petlyuk column

A systematic design procedure [32] for plant-wide control structure should have emphasis on the overall economic objective. For this study we use the following general economic objective [33]:

$$J = \text{cost of feed} - \text{value of products} + \text{cost of energy} \quad (2)$$

Fig. 1 shows the manipulated variables MV1, MV2, MV3, MV4, MV5, MV6, MV7, MV8, MV9 and MV10 used in designing control structure. The other manipulated variables not shown in Fig. 1 are distillate flow rate (D), bottoms flow rate (B) and condenser duty. They are used to control the liquid level in condenser and reboiler and, for vapor inventory control, respectively.

In this work, we use the six degrees of freedom in the pre-fractionator sub-columns C1, C21 and C22 to control the key impurities at their top and bottoms trays, to prevent them to escape as impurities in successive the sub-columns and hence in the final products.

Assuming all the products are about equally priced and that the price of energy is high, the final product purities are the active constraints as discussed by Skogestad [33]. In addition one may have constraints on individual impurities for side products. This leaves four degrees of freedom (MV7, MV8, MV9 and MV10) to control the “main” column, i.e., the sub-columns C31, C32 and C33. A multivariable controller would get even better performance, but our main objective is to show the feasibility, even with a simple structure.

In this work, we consider four decentralized control structures and evaluate their control performance for a wide range of disturbances like feed rate, feed compositions changes and feed vapor fraction.

The four control structures are named CS1, CS2, CS3 and CS4 for convenience. Simple decentralized proportional-integral (PI) controllers are used. The complete list pairing of controlled variables and manipulated variables used in the control structures are shown in Table 2.

Logarithmic transformation of compositions is used to reduce the effects of non-linearities [33,34]. Therefore, in control structures CS1, CS2 and CS4, controlled composition variables are actually  $\ln x_i$ , where  $x_i$  is the key impurity being controlled.

##### 5.1. Control structure 1 (CS1)

In control structure 1 (CS1), we implement the basic two point LV structure [33] on each sub-column where reflux (L) is used to control the key impurity in the top and vapor (V) is used to control the key impurity in the bottom. For example, in sub-column C1 (see Fig. 6), the key impurity on top tray is D (*n*-butanol) which is controlled using liquid reflux valve MV1.

**Table 2**

Pairing of manipulated variables with controlled variables in the four control structures a,b,c,d,e

MV <sup>b</sup>	Controlled variable			
	CS1 <sup>c</sup>	CS2 <sup>c</sup>	CS3	CS4 <sup>c</sup>
MV1	$x_D^a$ at C1 <sup>TOP</sup>	$x_D$ at C1 <sup>TOP</sup>	$T_{49}^{C1}$ <sup>d</sup>	$x_D$ at C1 <sup>TOP</sup> / $T_{12}^{C1,e}$
MV2	$x_A$ at C1 <sup>BTM</sup>	$x_A$ at C1 <sup>BTM</sup>	$T_{49}^{C1}$	$x_A$ at C1 <sup>BTM</sup> / $T_{12}^{C1,e}$
MV3	$x_C$ at C21 <sup>TOP</sup>	$x_C$ at C21 <sup>TOP</sup>	$T_{19}^{C21}$	$x_C$ at C21 <sup>TOP</sup> / $T_{19}^{C21,e}$
MV4	$x_D$ at C22 <sup>TOP</sup>	$x_D$ at C22 <sup>TOP</sup>	$T_{18}^{C22}$	$x_D$ at C22 <sup>TOP</sup> / $T_{18}^{C22,e}$
MV5	$x_A$ at C21 <sup>BTM</sup>	$x_A$ at C21 <sup>BTM</sup>	$T_{48}^{C21}$	$x_A$ at C21 <sup>BTM</sup> / $T_{48}^{C21,e}$
MV6	$x_B$ at C22 <sup>BTM</sup>	$x_B$ at C22 <sup>BTM</sup>	$T_{51}^{C22}$	$x_B$ at C22 <sup>BTM</sup> / $T_{51}^{C22,e}$
MV7	$x_B$ in condenser	$x_B$ in condenser	$T_{12}^{C31}$	$x_B$ at C31 <sup>TOP</sup> / $T_{12}^{C31,e}$
MV8	$x_C$ at C32 <sup>TOP</sup>	$x_C$ at C32 <sup>TOP</sup>	$T_{10}^{C32}$	$x_C$ at C32 <sup>TOP</sup> / $T_{10}^{C32,e}$
MV9	$x_D$ at C33 <sup>TOP</sup>	$x_D$ at C33 <sup>TOP</sup>	$T_{47}^{C33}$	$x_D$ at C33 <sup>TOP</sup> / $T_{47}^{C33,e}$
MV10	$x_C$ at reboiler	$x_C$ at reboiler+ $x_B$ at C32 <sup>BTM</sup> + $x_A$ at C31 <sup>BTM</sup>	$T_{56}^{C31}$	$x_C$ at reboiler+ $x_B$ at C32 <sup>BTM</sup> + $x_A$ at C31 <sup>BTM</sup>

<sup>a</sup>  $x$ : mole fraction; subscripts A: methanol, B: ethanol, C: propanol, D: *n*-butanol.  
<sup>b</sup> MV: manipulated variable.  
<sup>c</sup> Logarithm of  $x$  is used as controlled variable in CS1, CS2 and CS4; for example  $\ln(x_D)$  at C1<sup>TOP</sup> is paired with MV1 in control structures CS1, CS2 and CS4.  
<sup>d</sup>  $T$ : tray temperature; superscript: column section; subscript: tray number (numbered from top to bottom).  
<sup>e</sup> Temperature setpoints of slave controllers corrected by master composition controller.

At optimal (minimum energy) operation, sub-columns C31 and C32 have excess vapor for fractionation ( $V > V_{min}$ ) at the nominal feed conditions, thus a one-point control in these sections is sufficient [33]. Sub-columns C1, C21, C22 and C33 should be at their minimum vapor conditions ( $V = V_{min}$ ), therefore these column sections have two-point control.

5.2. Control structure 2 (CS2)

Structure CS2 is identical to CS1, except that for the loop involving the boilup (MV10). Note that in CS1, A (methanol) composition at the C31 bottom and B (ethanol) composition at C32 bottom are not controlled. Thus for certain disturbances, these light keys can

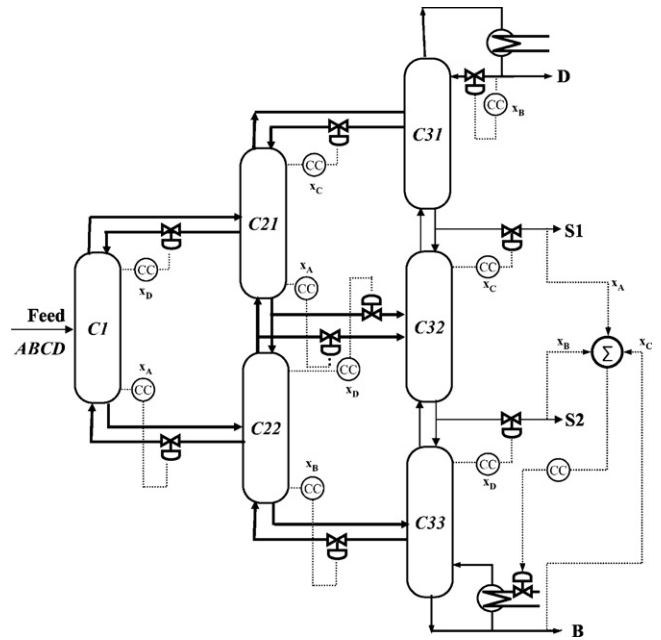


Fig. 7. Schematic of control structure 2 (CS2).

escape into the upper side product (S1) and lower side stream (S2) as impurity. This possibility is eliminated by ensuring that there is sufficient boilup for separation in the column sections C31 and C32. A simple way to ensure this, is to pair the boilup, MV10 (see Fig. 7) with sum of the light impurities at C31 bottom stage, C32 bottom stage and the C33 bottom stage (reboiler). Because the sum of the light keys is controlled with the boilup (MV10), there may be a small offset in the product purities.

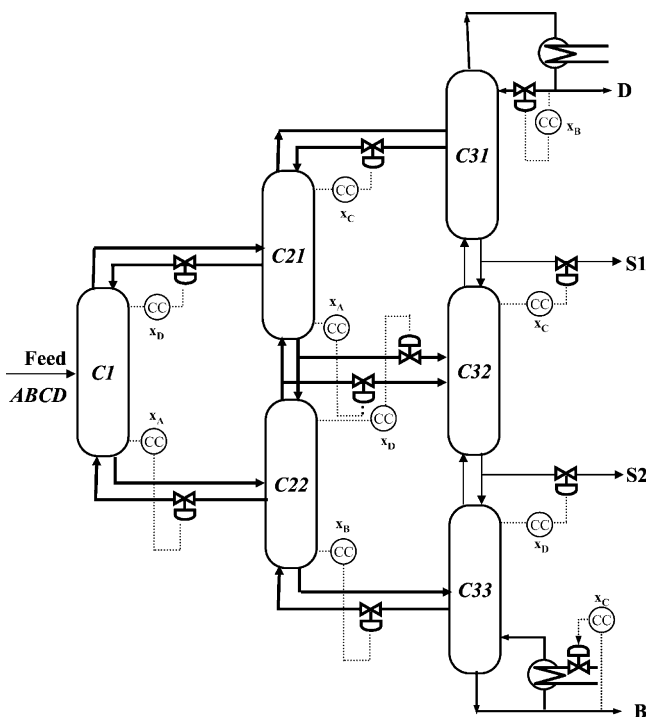


Fig. 6. Schematic of control structure 1 (CS1).

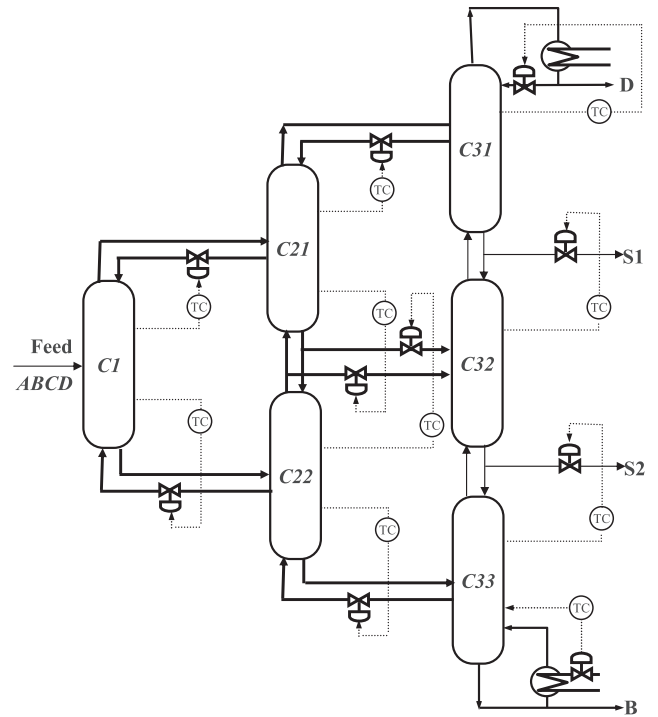


Fig. 8. Schematic of control structure 3 (CS3).

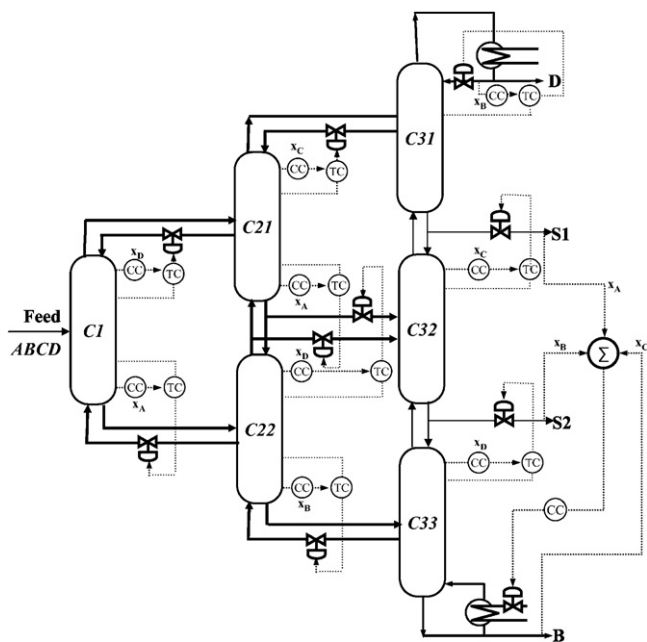


Fig. 9. Schematic of control structure 4 (CS4).

### 5.3. Control structure 3 (CS3)

This structure uses temperatures only, thus the idea is to infer compositions from temperature, which is not unique for multicomponent mixtures (see Fig. 8). The controlled variables are a sensitive stage temperature in the stripping and rectifying sections of sub-columns C1, C21, C22 and C33, respectively (see Table 2 for details). Note that, there is only one temperature control loop in columns C31 and C32.

### 5.4. Control structure 4 (CS4)

This is a modification of CS3, with the addition of several outer composition loops. The temperature setpoints of slave temperature controllers are set by master composition controller. The master composition loops control the same key impurities as in structures CS1 and CS2. For example, in sub-column C1, the setpoint of the top temperature controller is set by a master composition controller that controls the D (*n*-butanol) at top stage of column section C1. In addition, a modification same as the structure CS2 is that, the boilup (see Fig. 9) controls sum of the light impurities at C31 bottom stage, C32 bottom stage and the C33 bottom stage (reboiler).

## 6. Tuning

The tuning of the decentralized control structures was done using the SIMC tuning rules [35]. Because of the mainly sequential sequence of the columns, the controllers in the prefractionator sub-columns (C1, C21 and C22) are first closed. This is followed by the controllers in main column (C31, C32 and C33). Step changes in manipulated variables are made to identify the input–output steady state gain and dynamics. Most of the responses have only a small effective delay. The SIMC tuning factor,  $\tau_c$  was selected to get a smooth response (see Table 3).

## 7. Closed-loop simulation results

The proposed control structures were simulated with disturbances in feed rate, feed composition, feed vapor fraction and as well as product composition setpoint changes. The performance

Table 3  
SIMC tuning parameter ( $\tau_c$ ) used in the four control structures.<sup>a</sup>

Loop	CS1	CS2	CS3	CS4 <sup>a</sup>
MV1	5 min	5 min	5 min	4 min
MV2	3 min	3 min	3 min	4 min
MV3	5 min	5 min	5 min	4 min
MV4	5 min	5 min	5 min	4 min
MV5	3 min	3 min	3 min	8 min
MV6	3 min	3 min	3 min	8 min
MV7	20 min	20 min	5 min	12 min
MV8	20 min	20 min	5 min	8 min
MV9	20 min	20 min	5 min	8 min
MV10	5 min	5 min	3 min	5 min

<sup>a</sup>  $\tau_c$  for the master composition controllers;  $\tau_c$  for slave temperature controllers is same as in CS3 but without integral action.

is analyzed by considering the response in the final product compositions as well as product flows (D, S1, S2 and B) and energy usage (*V*). The minimum theoretical boilup ( $V_{min}$ ) required for sharp separation, for a new feed disturbance is also shown in the figures. Table 4 shows the summary of closed-loop responses using different control structures.

### 7.1. Performance of CS1 and CS2

Fig. 10, shows the closed-loop response for various feed disturbances, in the sequence as listed in Table 4. For a feed rate disturbance of +10% ( $t=0$ , Fig. 10), all the product purities are restored and the molar flows of products increase from a nominal flow rate of 0.25 mol/min to 0.275 mol/min. This is followed by various feed composition disturbances.

At  $t=7200$  min, we give changes in feed composition of components C (propanol) and D (*n*-butanol). The product purities of upper side product ( $x_B^{S1}$ ) deteriorate significantly and shows a long settling time. A similar deterioration in the product purity of S1 is seen in the figure at time,  $t=9600$  min, for a disturbance affected by increasing the vapor fraction of the feed by 20%. As explained in Section 2.1, the two side products have two key impurities. Since the light key on C31 bottom tray is not controlled, it can leak into the side product 1 (S1) for certain disturbances. These responses are discussed in more detail later in Section 8.1. Fig. 11 shows the performance for setpoint changes of +5% in the heavy keys of products D, S1 and S2 (at  $t=0$ , 1200 and 2400, respectively) using CS1.

Fig. 12 shows the closed-loop response using CS2 for a feed rate and feed composition disturbances. At  $t=0$ , we give a feed rate disturbance and the purities of four products can be restored like CS1. Unlike CS1, the purities of all the products including the upper side product ( $x_B^{S1}$ ) can be restored for all the feed composition

Table 4  
Summary of closed-loop response using different control structures.<sup>a,b,c</sup>

Disturbance <sup>c</sup>	CS1	CS2	CS3	CS4
Feed, +10%	OK	OK	OK	OK
$z_1^F$ (mol%) = [20 30 25 25]	OK	OK	OK	OK
$z_2^F$ (mol%) = [20 25 30 25]	OK	OK	OK	OK
$z_3^F$ (mol%) = [20 25 25 30]	OK	OK	Fail	OK
$z_4^F$ (mol%) = [25 20 30 25]	OK	OK	OK	OK
$z_5^F$ (mol%) = [25 25 20 30]	Fail	OK	Fail	OK
$z_6^F$ (mol%) = [25 20 25 30]	OK	OK	Fail	OK
+20% feed vapor fraction	Fail	OK	Fail	OK
$x_B$ in condenser, +5%	OK	OK	–	OK
$x_4^{S1}$ , +5%	OK	OK	–	OK
$x_2^{S2}$ , +5%	OK	OK	–	OK

<sup>a</sup> OK: closed-loop stable and purity of all products restored.

<sup>b</sup> Fail: closed-loop stable but purity of upper side product is not maintained ( $x_B^{S1}$  dropped considerably).

<sup>c</sup> Nominal feed rate:  $F=1$  mol/min  
Nominal feed composition,  $z_F$  (mol%) = [25 25 25 25] (equimolar).

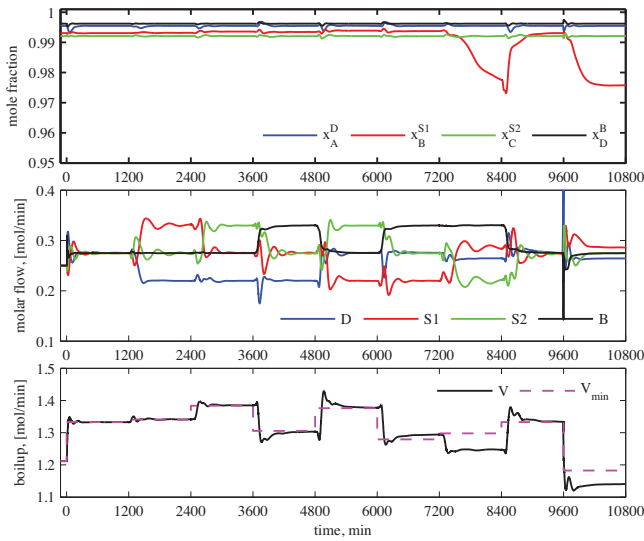


**Fig. 10.** CS1: closed-loop results for feed disturbances. Purity of upper side product ( $x_B^{S1}$ ) drops at time 7200 and 9600 (**not acceptable**).

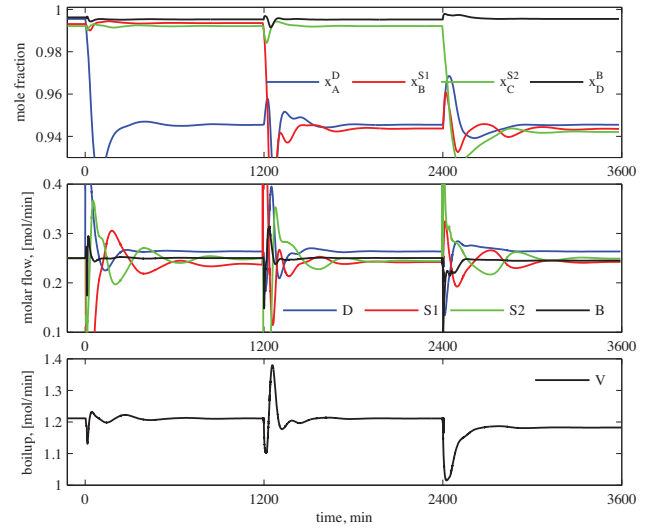


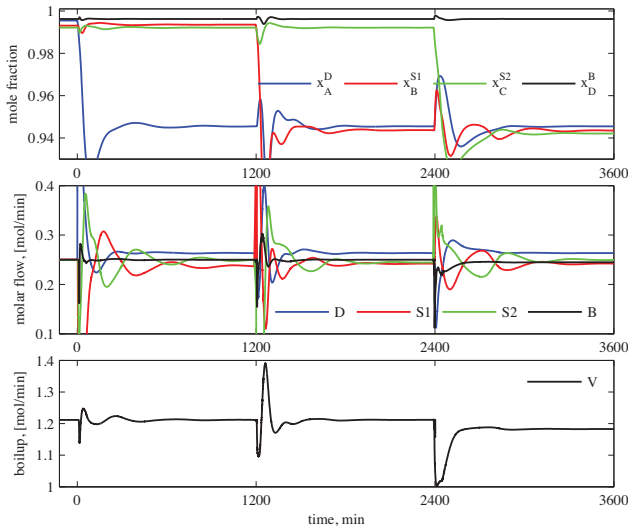
**Fig. 13.** CS2: closed-loop results for setpoint changes.

disturbances. In Fig. 13, we show a +5% composition setpoint changes in the heavy keys of products D, S1 and S2.

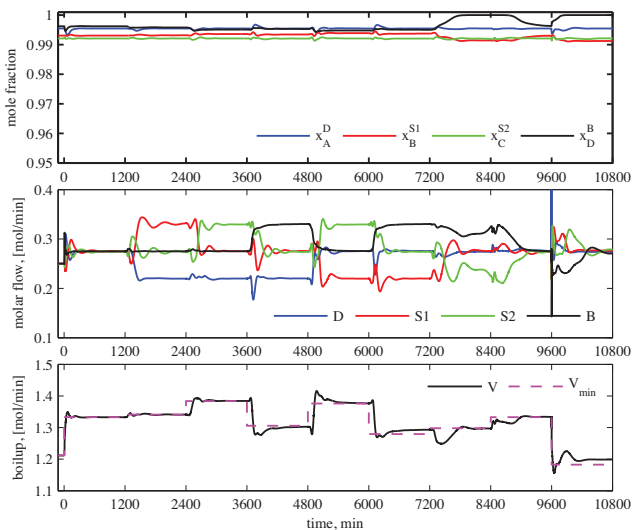
### 7.2. Performance of CS3 and CS4

Fig. 14 shows the response for a feed rate increase by 10%, at  $t=0$ . All the product purities are restored and the molar flows of products increase from a nominal flow rate of 0.25 mol/min to 0.275 mol/min. Since we are studying a multicomponent separation, for feed composition changes, temperature control alone may not be sufficient for sharp separation. For example, the closed-loop response for a feed composition disturbance in components A (methanol) and D (*n*-butanol), at  $t=3600$ , there is a large deterioration in the product purity of upper side product ( $x_B^{S1}$ ). For this disturbance, the energy usage is more than the “minimum or  $V_{min}$ ”. There is a similar deterioration in purity of S1 for the feed vapor fraction disturbance at  $t=9600$ , for which the energy loop decreases the boilup, less than the  $V_{min}$ .

The control structure CS4 uses composition/temperature cascade controllers. Note that unlike the response using structure CS1



**Fig. 11.** CS1: closed-loop results for setpoint changes.



**Fig. 12.** CS2: closed-loop results for feed disturbances.

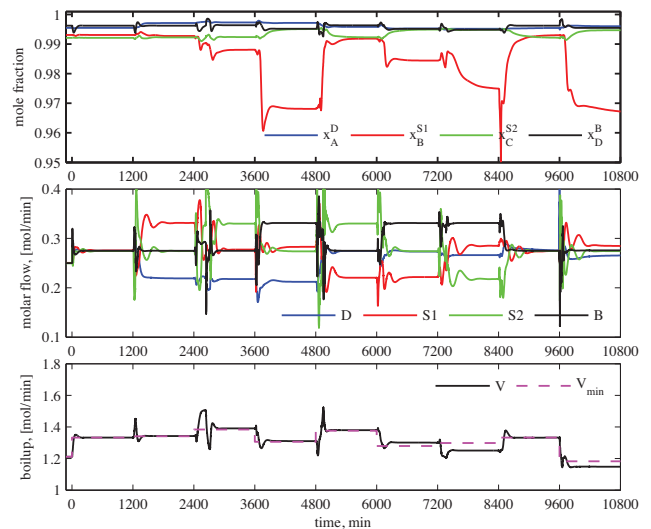


**Fig. 14.** CS3: closed-loop results for feed disturbances. Purity of upper side product ( $x_B^{S1}$ ) drops at time = 3600, 4800, 6000, 7200 and 9600 (**not acceptable**).

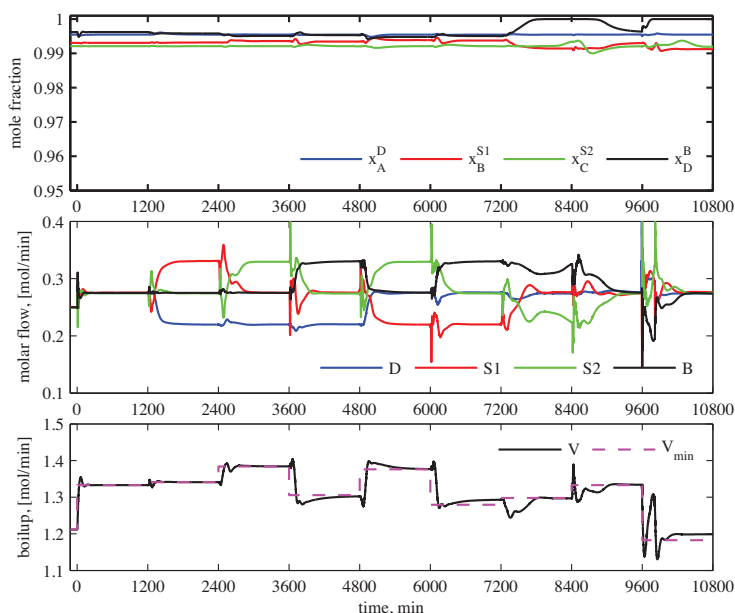


Fig. 15. CS4: closed-loop results for feed disturbances.

(see Fig. 10) and structure CS3 (see Fig. 14), purity of all the products can be restored after initial transient. Fig. 15 shows that all the disturbances under study can be rejected and product purities are restored. Similarly, Fig. 16 shows composition setpoint changes in products D, S1 and S2.

## 8. Discussion

### 8.1. Impact of feed disturbances and the $V_{min}$ diagram

As discussed in Section 7.1, the closed-loop responses were stable for all disturbances using CS1. However, for a feed composition disturbance with 20% C (propanol) and 30% D (*n*-butanol), although the response was closed-loop stable, the purity of

upper side product ( $x_B^{S1}$ ) deteriorated considerably (see Fig. 10, at  $t=7200$  min). A similar deterioration in the purity of upper side product (see Fig. 10, at  $t=9600$  min) is seen when the vapor fraction was increased by 20%. This can be explained using the “ $V_{min}$ ” tool.

Fig. 17 shows the  $V_{min}$  diagram for nominal feed mixture, in solid lines. As explained in Section 3, the minimum boilup for sharp separation is set by the “most difficult binary split”. This is denoted in Fig. 17 by peak points  $P_{AB}$ ,  $P_{BC}$  and  $P_{CD}$ . For the nominal feed, the peak  $P_{CD}$  is highest. This implies that the separation of C/D is the most difficult. For separation of this feed using the Petlyuk arrangement, the minimum boilup is set by this split.

At an operating point close to minimum energy, the sub-column C33 (doing C/D split) is at the limiting reflux while sub-columns C32

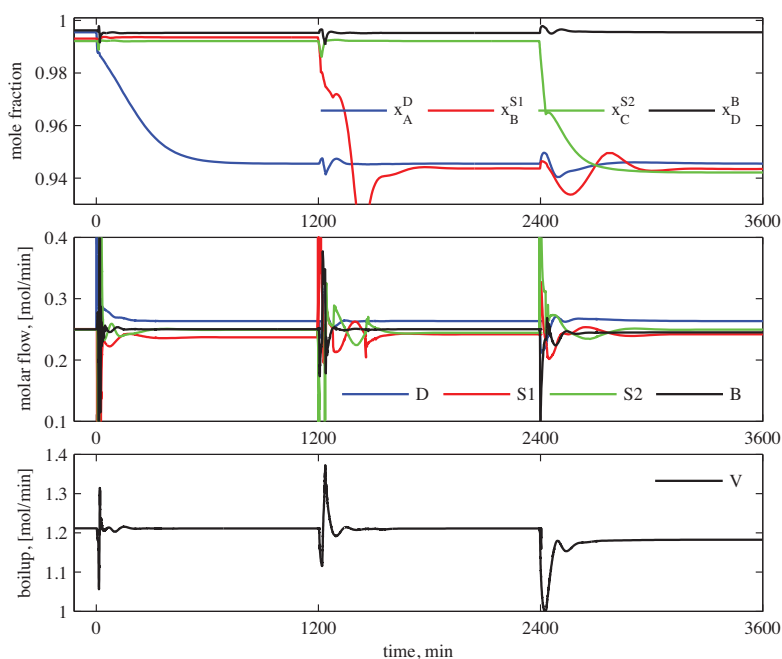
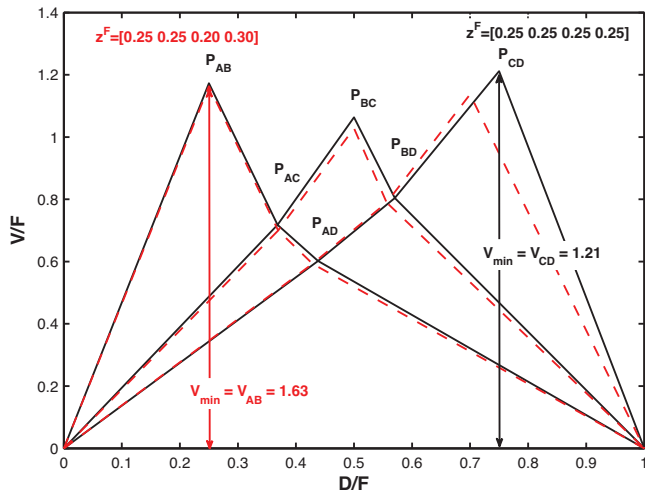


Fig. 16. CS4: closed-loop results for setpoint changes.





**Fig. 17.**  $V_{min}$  diagrams: nominal feed composition,  $z^F$  (mol%) = [25 25 25 25] (solid line)  $z^F$  (mol%) = [25 25 20 30] (dashed line).

and C31 have some excess reflux. Because the sub-column C33 has a two point control in structure CS1, for any disturbance that does not cause change the order of these peaks, structure CS1 can give pure side products. In other words, a disturbance that may cause A/B or B/C split to demand more boilup that the C/D split, the upper side product (S1) or the lower side product (S2) may become impure, respectively.

Fig. 17 shows the  $V_{min}$  plot (in dashed line) for a new feed composition with 20% C and 30% D. Now, peak  $P_{AB}$  is highest, which makes the A/B separation the most difficult split. The structure CS1 has only one point control of sub-column C31. There is an insufficient boilup for a A/B separation and A (methanol) escapes from the bottom tray of column section C31, to contaminate the upper side product (S1). The similar reasoning can be given for a feed vapor fraction disturbance. See Fig. 18, there is a change in the order peak points, resulting in the drop in the purity of upper side product (S1).

For the disturbances leading to changes in the peaks in  $V_{min}$  diagrams, a maximum-select controller with boilup can be used to implement a two point control in sub-columns C31, C32 and C33. Alternately in CS2 and CS4, we propose a single controller that pairs

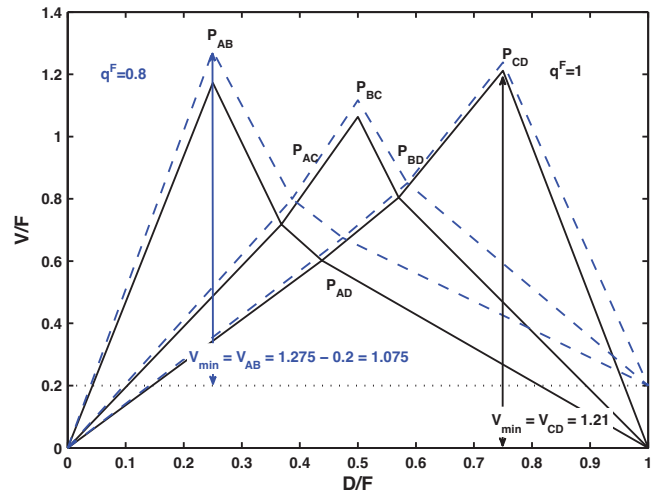


**Fig. 18.**  $V_{min}$  diagrams: nominal feed vapor fraction,  $q^F = 1$  (solid line) and for  $q^F = 0.8$  (dashed line).

boilup with the sum of the composition of light impurities at the bottom stages of the sub-columns C31, C32 and C33.

## 8.2. Temperature control

The control structures CS3 and CS4 use temperature controllers. The most sensitive tray temperature corresponding to a manipulated variable is chosen as the control variable. The manipulated variables are perturbed in manual mode from steady state to identify the sensitive tray temperatures. Fig. 19 shows the effect of 1% change in reflux (MV1) to sub-column C1. The first plot shows the difference in the temperature of sub-column C1 from the initial state to the new steady state after perturbation. Tray 12 ( $T_{12}^1$ ) is clearly the most sensitive. The second plot shows the dynamics of tray temperature 12 of sub-column C1. This stage temperature ( $T_{12}^1$ ) is paired with MV1, and tuned for a good closed-loop response.

The control structure, CS3 uses temperature control alone. In a multi-component separation, the setpoints of temperature controllers should be changed for the feed composition disturbances. Figure (see Fig. 14, at  $t = 3600$  min) shows the regulatory response using CS3 when the composition of the components A

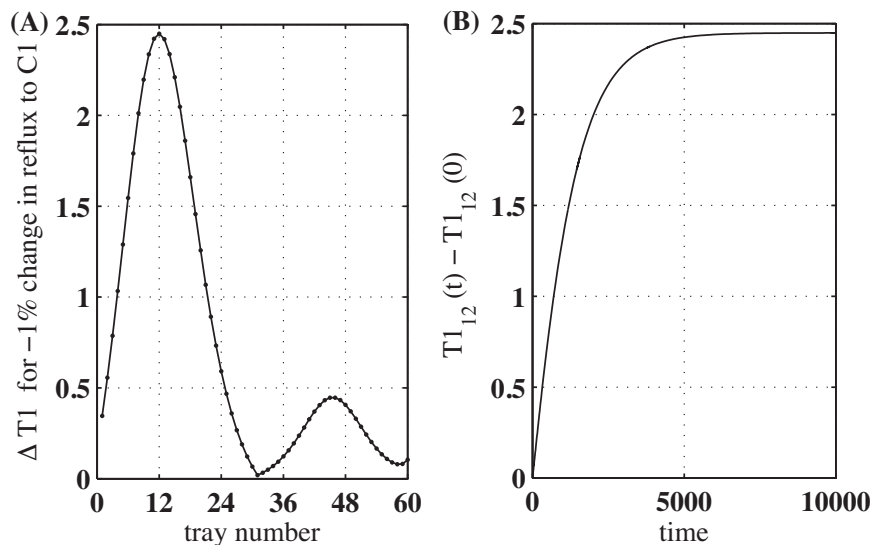


**Fig. 19.** (A) Change in temperatures of column section, C1 for -1% change in reflux. (B) Column C1, tray 12 temperature ( $T_{12}^1$ ) for -1% change in reflux to C1.

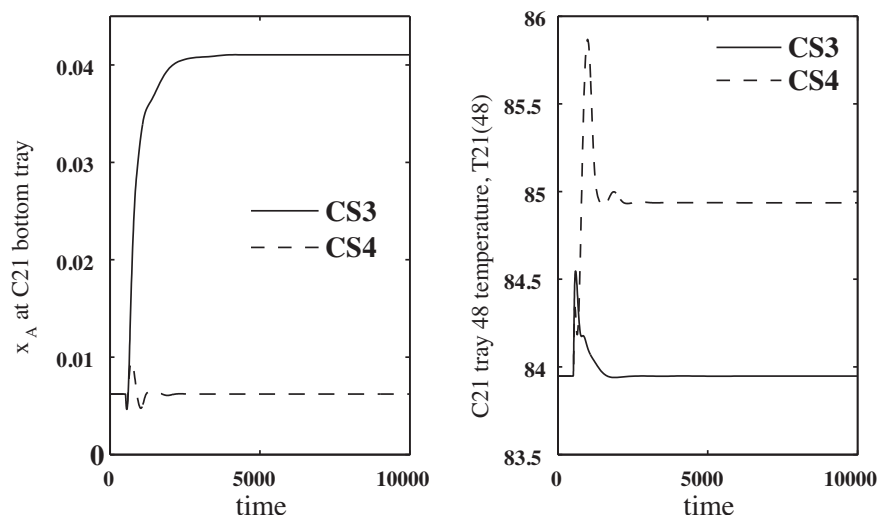


Fig. 20. Regulatory response using CS3 and CS4 for a feed composition of  $z^F$  (mol%) = [20 25 25 30] on prefractionator column (C21) separation.

(methanol) and D (*n*-butanol) in feed is changed. The purity of upper side product ( $x_B^{S1}$ ) drops considerably. As temperature setpoint of the controller is constant, a significant amount of A (methanol) escapes the sub-column C21 bottoms and appears in upper side product (S1) as impurity.

For a feed composition change from a nominal equimolar feed to one containing 20% A and 30% D, Fig. 20 shows the composition of A (methanol) at the bottom tray of sub-column C21 using control structures CS3 and CS4. The second subplot shows the temperature of tray 48 in C21, which is paired with manipulated variable MV5. In structure CS4, the setpoint of the slave temperature controller is corrected using a master composition controller, which controls A (methanol) at the C21 bottom stage at its nominal value. Any key impurities escaping from sub-columns C1, C21 and C22 may make the final product impure. However for feed rate changes with fixed composition, the temperature control alone may be sufficient.

### 8.3. Composition control

The prefractionator “sub-column” C1 separates the components A and D. We thus control *n*-butanol,  $x_D$  (heavy impurity) in the top (or more precisely in the liquid on the top stage) and methanol,  $x_A$  (light impurity) in the bottom liquid product. The optimal purities may vary and/or be difficult to find, but since this is an easy separation and we assume a relatively large number of stages. It will not cost much energy to over-fractionate, so it is suggested to set the setpoints for  $x_A$  and  $x_D$  at low values (for example,  $10^{-4}$ ). Similarly, in sub-column C21 we control the key components A (methanol) and propanol (C), and in column C22 we control key components B (ethanol) and D (*n*-butanol). Again, the setpoints for these may be set to low values, because the separations are expected to be easy compared to the number of stages.

For the sub-columns C31, C32 and C33, with the four end products, the choice on control variable is more difficult. For the top three products (D, S1 and S2), we suggest to control the corresponding heavy key impurity ( $x_B$ ,  $x_C$  and  $x_D$ , respectively) at the top stage in each sub-columns, by manipulating the liquid reflux into these sub-columns. The setpoints for these impurities are set by product specifications or by optimization. Three light key impurities now remain uncontrolled; namely  $x_C$  in the bottom product (B),  $x_B$  in the lower side product (S2) and  $x_A$  in the upper side product (S1). However, these three impurities cannot be controlled independently [7] because they are all determined by the boilup (V),

which sets the vapor flow in the sub-columns C31, C32 and C33. The standard solution to this is to have three composition controllers (and three setpoints) with a max-selector that implements the largest controller output (boilup). This will imply that two of the products are over-purified. Alternatively, we propose a simpler solution with only one controller, which is to control the sum of the impurities,  $\ln(x_A + x_B + x_C)$ . The setpoint of this sum can then be adjusted to achieve the desired purities of the “limiting” product. Notice that when the boilup is used to control the sum of the light keys (in control structures CS2 and CS4), for the disturbances making A/B becomes the most difficult split (at time = 7200, 9600 in Figs. 12 and 15), the bottom product gets over-purified, while other products are at their specifications.

There may also be a possibility of infeasibility in the setpoints of the key impurities in the two-point control of sub-columns. But this is eliminated by the choice of large number of stages. Another problem using composition control of keys at the column ends with composition pinch zones is that, the steady state gain for the corresponding manipulated variable can be nearly zero and there may be strong non-linearity effects as also discussed by previous workers [36,37]. Therefore, their control using a feed back controller can be impossible. For sub-columns with limiting internal flows, there are no composition pinch zones at the ends and consequently, there is a large steady state gain with the manipulated variables. Therefore, composition control is feasible with a feedback controller. However, in the sub-column C32 because of excess internal vapor and liquid flows (see Fig. 3), there is a long pinch in the stripping section. B (ethanol) at C32 bottom tray was not chosen as a controlled variable, because of severe non-linearity effects. A composition on a sensitive tray and not a tray in the pinch zone can be a better candidate control variable.

## 9. Conclusions

In this paper, we propose simple decentralized control structures for minimum energy operation of the four-product Petlyuk column arrangement shown in Fig. 1 or, its equivalent arrangement as shown in Fig. 2.

The proposed composition control scheme CS2 is shown in Fig. 7. It requires composition measurements or estimates for most internal and external flows in the column. If these composition measurements are not available, one may use the control structure CS4 in Fig. 9, where the inner temperature loops are

sufficient to stabilize the operation. The outer cascade composition loops are required in order to maintain product compositions and achieve minimum energy operation. The three prefractionator columns perform three easy splits (A/D, A/C and B/D), and the corresponding six key impurities may usually be controlled at low values without a noticeable increase in energy consumption. The remaining four degrees of freedom are used to control the three difficult splits (A/B, B/C and C/D) in the main column. We propose to control the amount of heavy impurity in the three light products (D, S1, S2) by adjusting the three liquid flows into the corresponding sections. Boilup ( $V$ ) is then left to control the light impurity in the three heavy products (S1, S2 and B), and, in accordance with the  $V_{min}$ -diagram, we propose to control the most difficult split, for example, by using boilup to control the “maximum” of the three impurities (control structure, CS4) or their sum (control structure, CS2). This will result in “over-purification” of two of the products, but this will not generally increase the energy consumption because, as known from the  $V_{min}$ -diagram, we will optimally have excess energy in two of the sections.

It may be possible to simplify the control structure by fixing some of the manipulated variables for example, some vapor splits, for a feed with a reasonably steady properties or when the product purity specifications are relaxed for some of the products. This should be investigated in detail for various feed mixtures and required purity specifications.

## References

- [1] F. Petlyuk, V. Platonov, D. Slavinskii, Thermodynamically optimal method for separating multicomponent mixtures, *International Chemical Engineering* 5 (1965) 555–561.
- [2] R.P. Cahn, A.G. DiMiceli, Separation of multicomponent mixture in single tower, United States Patent Office, US 3058893 (1962).
- [3] W. Stupin, Thermally coupled distillation – a case history, *Chemical Engineering Progress* 68 (1972).
- [4] G. Kaibel, Distillation columns with vertical partitions, *Chemical Engineering & Technology* 10 (1987) 92–98.
- [5] I. Dejanovic, L. Matijasevic, Z. Olujic, Dividing wall column – a breakthrough towards sustainable distilling, *Chemical Engineering and Processing: Process Intensification* 49 (2010) 559–580.
- [6] I.J. Halvorsen, S. Skogestad, Minimum energy consumption in multicomponent distillation. 3. More than three products and generalized Petlyuk arrangements, *Industrial & Engineering Chemistry Research* 42 (2003) 616–629.
- [7] E.A. Wolff, S. Skogestad, Operation of integrated three-product (Petlyuk) distillation columns, *Industrial & Engineering Chemistry Research* 34 (1995) 2094–2103.
- [8] G. Niggemann, C. Hiller, G. Fieg, Experimental and theoretical studies of a dividing-wall column used for the recovery of high-purity products, *Industrial & Engineering Chemistry Research* 49 (2010) 6566–6577.
- [9] F. Lestak, R. Smith, V. Dhole, Heat transfer across the wall of dividing wall columns, *Trans. Inst. Chem. Eng.* 72A (1994) 639–644.
- [10] M.I.A. Mutalib, A.O. Zeglam, R. Smith, Operation and control of dividing wall distillation columns: Part 2: Simulation and pilot plant studies using temperature control, *Chemical Engineering Research and Design* 76 (1998) 319–334.
- [11] H. Ling, W.L. Luyben, New control structure for divided-wall columns, *Industrial & Engineering Chemistry Research* 48 (2009) 6034–6049.
- [12] A.A. Kiss, C.S. Bildea, A control perspective on process intensification in dividing-wall columns, *Chemical Engineering and Processing: Process Intensification* 50 (2011) 281–292.
- [13] H. Ling, Z. Cai, H. Wu, J. Wang, B. Shen, Remixing control for divided-wall columns, *Industrial & Engineering Chemistry Research* 50 (2011) 12694–12705.
- [14] R.C. van Diggelen, A.A. Kiss, A.W. Heemink, Comparison of control strategies for dividing-wall columns, *Industrial & Engineering Chemistry Research* 49 (2010) 288–307.
- [15] T. Adrian, H. Schoenmakers, M. Boll, Model predictive control of integrated unit operations: control of a divided wall column, *Chemical Engineering and Processing* 43 (2004) 347–355.
- [16] R.R. Rewagad, A.A. Kiss, Dynamic optimization of a dividing-wall column using model predictive control, *Chemical Engineering Science* 68 (2012) 132–142.
- [17] C. Buck, C. Hiller, G. Fieg, Applying model predictive control to dividing wall columns, *Chemical Engineering & Technology* 34 (2011) 663–672.
- [18] Z. Olujic, M. Jödecke, A. Shilkin, G. Schuch, B. Kaibel, Equipment improvement trends in distillation, *Chemical Engineering and Processing: Process Intensification* 48 (2009) 1089–1104.
- [19] I. Dejanovic, L. Matijasevic, I. Halvorsen, S. Skogestad, H. Jansen, B. Kaibel, Olujic, Designing four-product dividing wall columns for separation of a multicomponent aromatics mixture, *Chemical Engineering Research and Design* 89 (2011) 1155–1167.
- [20] R. Agrawal, Z.T. Fidkowski, More operable arrangements of fully thermally coupled distillation columns, *AIChE Journal* 44 (1998) 2565–2568.
- [21] D. Dwivedi, I. Halvorsen, S. Skogestad, Control structure design for optimal operation of thermally coupled columns, in: *Heritage Distillation Symposium*. Dr James Fair. Topical Conference at the 2011 AIChE Spring Meeting, Curran Associates Inc, 2011.
- [22] I.J. Halvorsen, S. Skogestad, Minimum energy consumption in multicomponent distillation. 1.  $V_{min}$  diagram for a two-product column, *Industrial & Engineering Chemistry Research* 42 (2003) 596–604.
- [23] A.J.V. Underwood, Fractional distillation of multicomponent mixtures, *Industrial & Engineering Chemistry* 41 (1949) 2844–2847.
- [24] I. Dejanovic, L. Matijasevic, I.J. Halvorsen, S. Skogestad, H. Jansen, B. Kaibel, Z. Olujic, Designing four-product dividing wall columns for separation of a multicomponent aromatics mixture, *Chemical Engineering Research and Design* 89 (2011) 1155–1167.
- [25] M. Ghadrddan, I.J. Halvorsen, S. Skogestad, A shortcut design for Kaibel columns based on minimum energy diagrams, in: *21st European Symposium on Computer Aided Process Engineering*, vol. 29 of *Computer Aided Chemical Engineering*, Elsevier, 2011, pp. 356–360.
- [26] I.J. Halvorsen, S. Skogestad, Minimum energy consumption in multicomponent distillation. 2. Three-product Petlyuk arrangements, *Industrial & Engineering Chemistry Research* 42 (2003) 605–615.
- [27] Z. Fidkowski, L. Królikowski, Minimum energy requirements of thermally coupled distillation systems, *AIChE Journal* 33 (1987) 643–653.
- [28] V. Alstad, Studies on selection of controlled variables, Ph.D. Thesis, Norwegian University of Science and Technology, Department of Chemical Engineering, 2005.
- [29] A.C. Christiansen, Studies on optimal design and operation of integrated distillation arrangements, Ph.D. Thesis, Norwegian University of Science and Technology, Department of Chemical Engineering, 1997.
- [30] I.J. Halvorsen, S. Skogestad, Optimal operation of Petlyuk distillation: steady-state behavior, *Journal of Process Control* 9 (1999) 407–424.
- [31] A.A. Kiss, R.R. Rewagad, Energy efficient control of a btx dividing-wall column, *Computers & Chemical Engineering* 35 (2011) 2896–2904.
- [32] S. Skogestad, Plantwide control: the search for the self-optimizing control structure, *Journal of Process Control* 10 (2000) 487–507.
- [33] S. Skogestad, The do's and don'ts of distillation column control, *Chemical Engineering Research and Design* 85 (2007) 13–23.
- [34] S. Skogestad, M. Morari, LV-control of a high-purity distillation column, *Chemical Engineering Science* 43 (1988) 33–48.
- [35] S. Skogestad, Simple analytic rules for model reduction and pid controller tuning, *Journal of Process Control* 13 (2003) 291–309.
- [36] C. Fuentes, W.L. Luyben, Control of high-purity distillation columns, *Industrial & Engineering Chemistry Process Design and Development* 22 (1983) 361–366.
- [37] J.S. Moczek, R.E. Otto, T.J. Williams, Control of distillation column for producing high-purity overheads and bottoms streams, *Industrial & Engineering Chemistry Process Design and Development* 2 (1963) 288–296.